Supporting Information

Downregulating Scar Formation by Microneedle Directly *via* Mechanical Communication Pathway

*Qing Zhang, Lin Shi, Hong He, Xingmou Liu, Yong Huang, Dan Xu, Mengyun Yao, Ning Zhang, Yicheng Guo, Yifei Lu, Haisheng Li, Junyi Zhou, Jianglin Tan *, Malcolm Xing *, Gaoxing Luo**

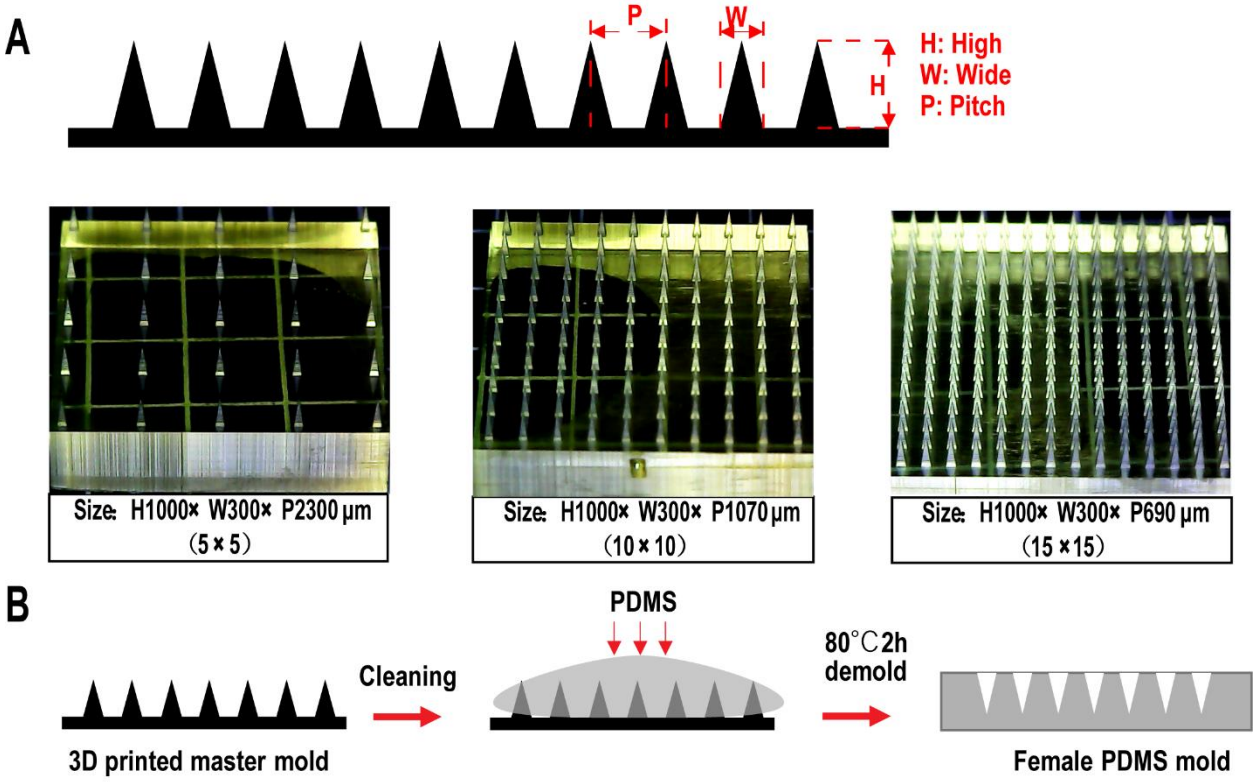

Figure S1. Microneedles (MNs) molds. (A) Three different positive molds with array of 5×5, 10×10 and 15×15 manufactured by 3D printer. (B) Illustration of PDMS negative mold manufacturing.

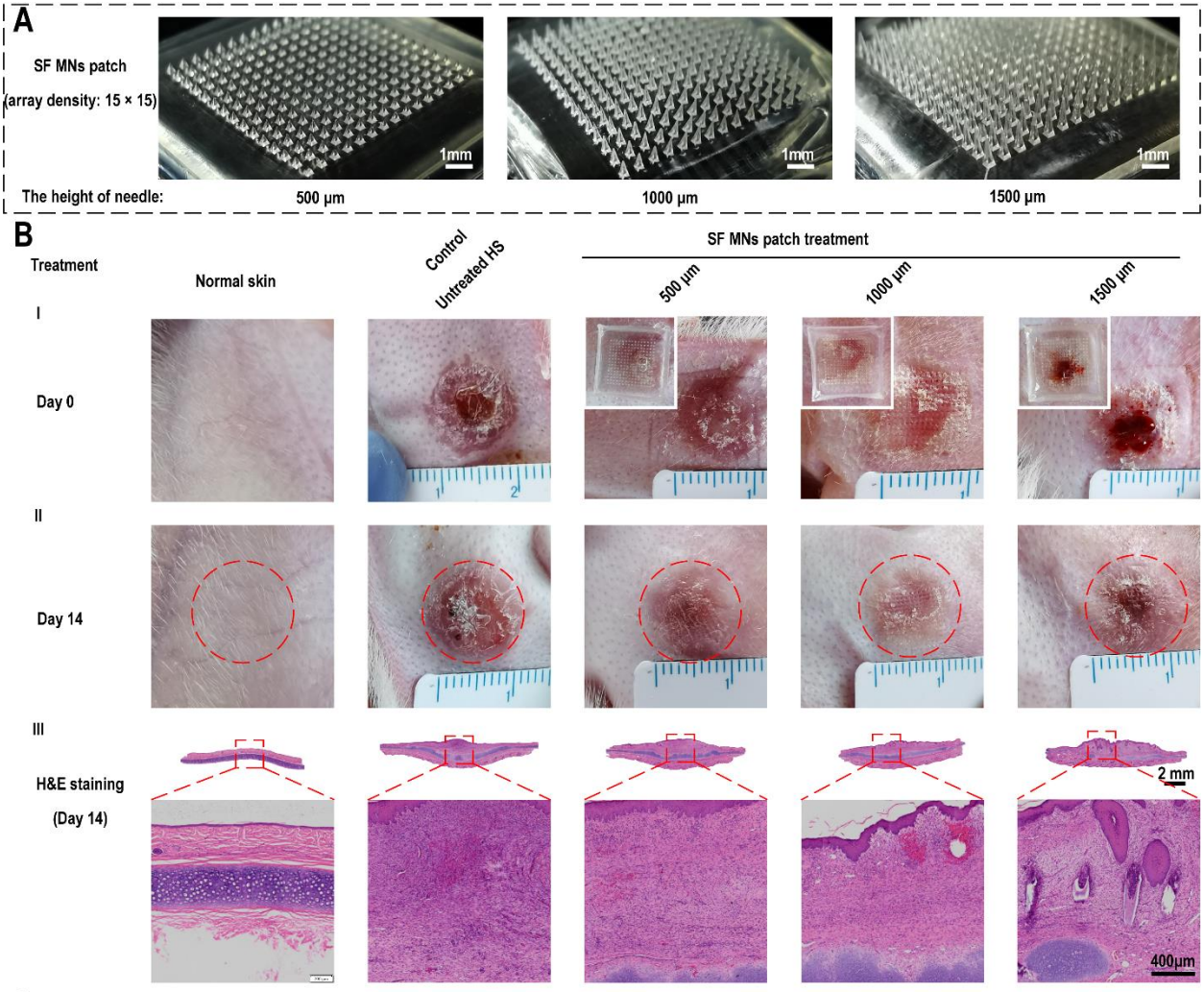

C

	Normal skin	Control (untreated HS)	SF MNs treated HS		
			500 μm	1000 μm	1500 μm
Thickness of tissue above the cartilage / μm	400.27 ±14.26	1943.62 ±232.28	1709.41 ±570.384	1178.26 ±79.84	1654.15 ±293.44
Scar elevation index (SEI)	1.03 ±0.07	4.61 ±0.83	4.21 ±0.76	2.67 ±0.39	3.79 ±0.80

Figure S2. Therapeutic efficacy on HS of microneedles patch in different sizes. (A) Three different sizes of SF MNs (500 μm, 1000 μm and 1500 μm in height) were designed and fabricated. Scale bar, 1 mm (B) 500 μm MNs were too short to achieve an efficient penetration. With the increasing length of needle, the penetration improved. However, there were adverse effects such as bleeding and inflammatory response for the group of 1500 μm

MNs (I). After two weeks of treatment, the normal skin and HS tissues were harvested (II) and stained with H&E (III). Scale bar, 2 mm and 400 μm. (C) The therapeutic efficacy was evaluated in the thickness of HS tissues and scar elevation index (SEI). Compared to the limited therapeutic efficacy of 500 μm MNs (thickness: 1709.41 ± 570.38 μm, SEI: 4.21 ± 0.76), significant improvements were achieved in the group of 1000 μm (thickness: 1178.25 ± 79.84 μm, SEI: 2.67 ± 0.39), which was also slightly better than group of 1500 μm (thickness: 1654.15 ± 293.44 μm, SEI: 3.79 ± 0.80).

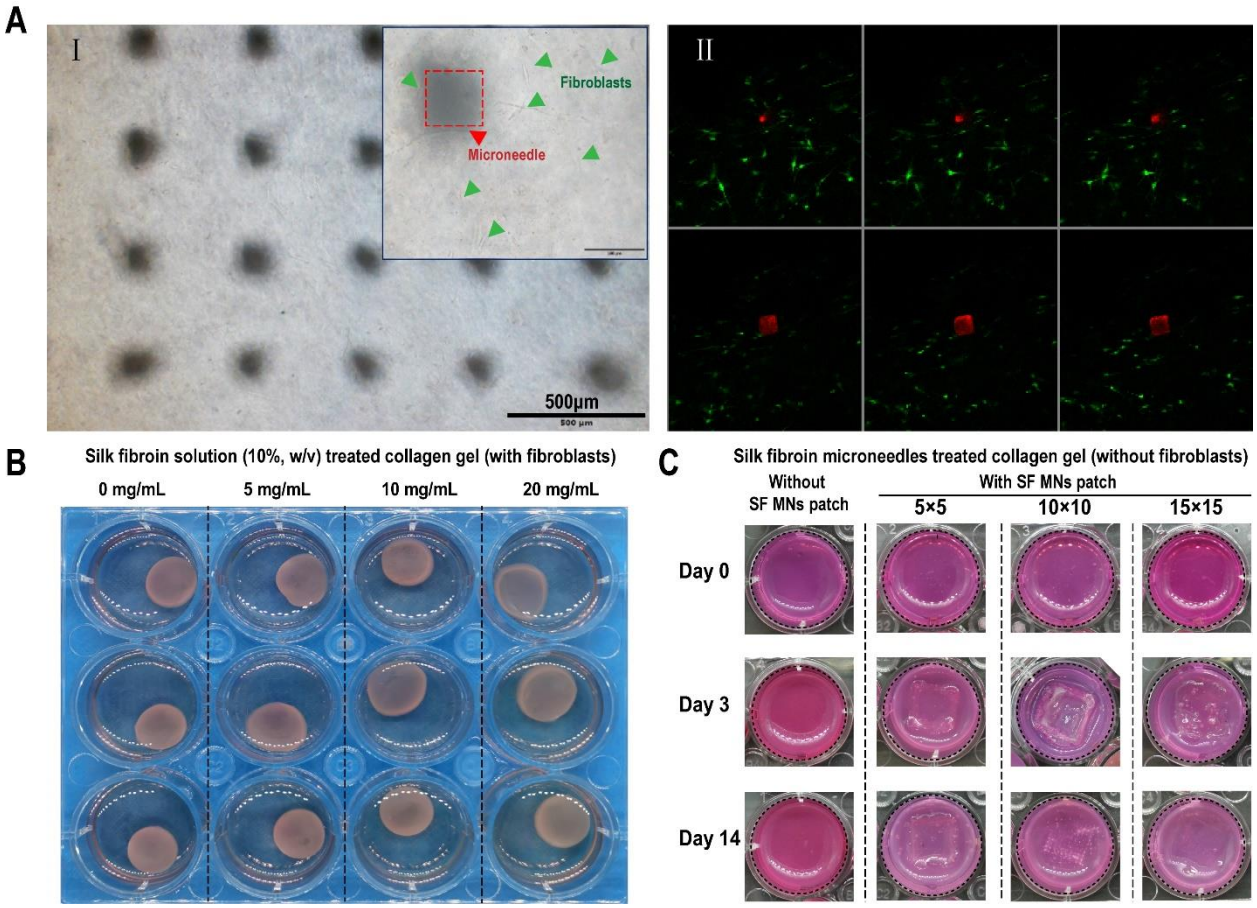

Figure S3. Fibroblast-populated collagen lattice system (FPCL). (A) Coexistence state between cells and SF MNs characterized by optical microscope (I) and confocal laser scanning microscope (II), respectively. (B) SF solution (10%, w/v) had no inhibition on the contraction of HSFs in FPCL system at the dosage range from 0 to 20 mg/mL, a SF MNs patch is equivalent to containing 100μL SF solution (10%, w/v). (C) The blank collagen gel (without fibroblasts) would not contract regardless whether there is a microneedles patch.

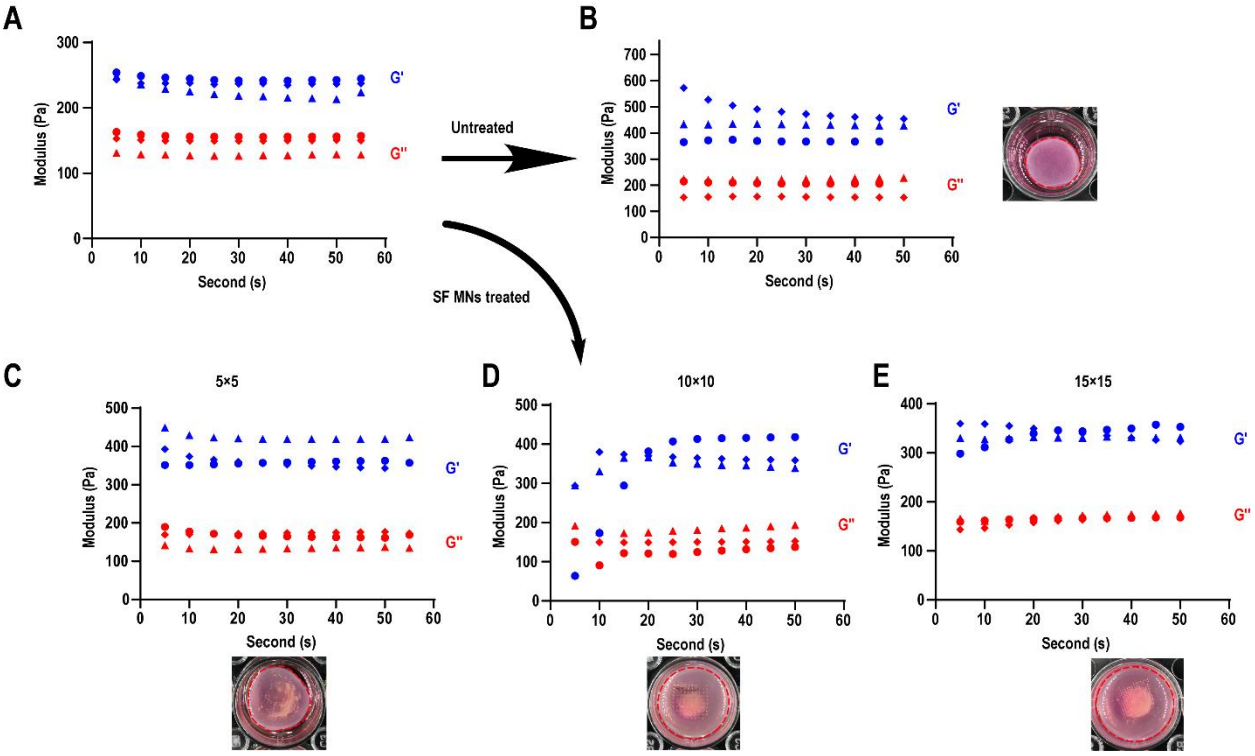

Figure S4. Mechanical properties of the collagen hydrogel in FPCL. The storage modulus (G′) increased with contraction. *n* = 3. (A) The initial G′ of collagen hydrogel. (B) After 14 days of culture, the changes in G′ of collagen hydrogel in the control group (untreated), and SF MNs treated groups with array of (C) 5 × 5, (D) 10 × 10, (E) 15 × 15.

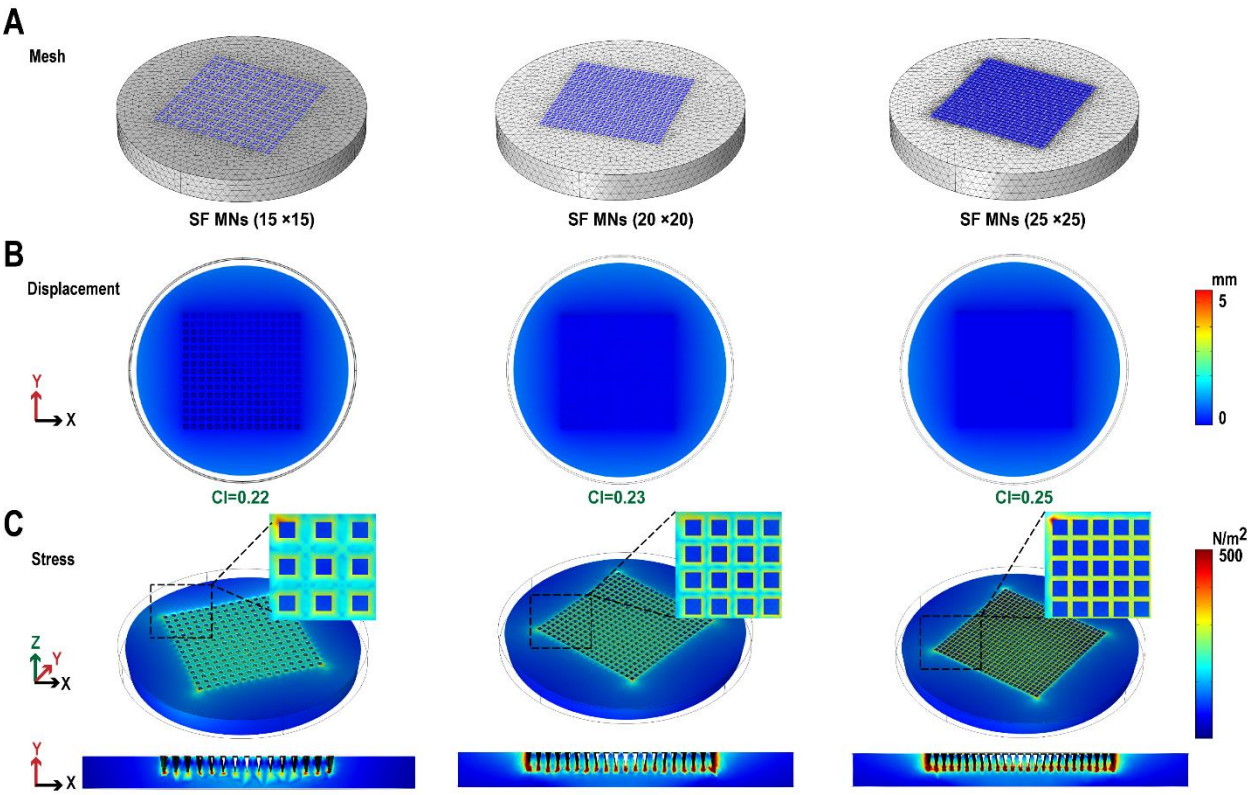

Figure S5. Further finite element study on the situations with higher MNs array density, The contraction index (CI) marginally increased while the array density exceeded 20×20. Additionally, higher mechanical stress tends to concentrate at microneedles patch embedded sites during contraction with the increasing array density. (A) Meshed FPCL system. (B) Collagen contraction and the simulated CI. (C) 3D and section contour of Von Mises stress.

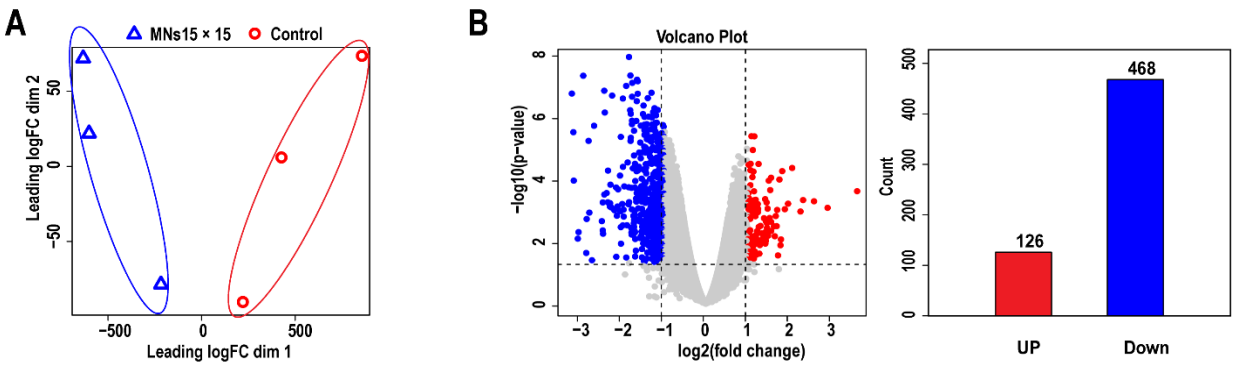

Figure S6. RNA sequencing analysis of cellular responses to the SF MNs intervention in FPCL system. (A) Principal component analysis (PCA) was performed based on differentially expressed genes (DEGs) between control (untreated group) and SF MNs treated group. (B) Volcano plots showing the 126 up-regulated and 468 down-regulated genes in response to SF MNs treatment.

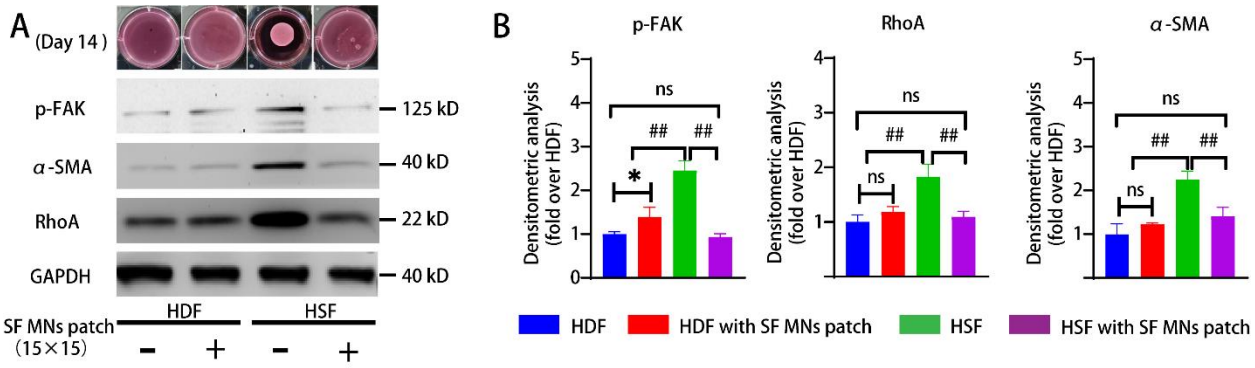

Figure S7. SF MNs intervention resulted in significant different changes in contraction, and expression of pFAK, RhoA and α-SMA in normal human dermal fibroblasts (HDFs) and human scar fibroblasts (HSFs). (A) Collagen contraction in groups of HDFs and HSFs with or without the treatment SF MNs, and western blotting of expression levels of the proteins. (B) Semi-quantitative statistics of protein levels from western blotting. $p^{*} < 0.05$ compared with HDF, $p^{\#\#} < 0.01$ compared with HSF, n = 3.

Table S1. Secondary structure content of natural silk fibroin (SF) and methanol treated SF. The bolded numbers indicate significant changes in content of β-sheet between the natural and methanol treated SF.

Secondary structure fractions	Natural silk fibroin		Methanol treated silk fibroin	
	Peak position(cm^{-1})	Area (%)	Peak position(cm^{-1})	Area (%)
Random coil / α-helix (1635–1664 cm^{-1})	1645 1664	131.7 (45.1%) 59.9 (20.5%)	1663	344.2 (39.8%)
β-sheet **1620 – 1630 cm−1 / 1690 -1700 cm−1**	**1622** **1693**	**55.9** **(19.1%)** **19.0** **(6.5%)**	**1627**	**521.2** **(60.2%)**
β-turn (1666-1690 cm^{-1})	1679	25.8 (8.8%)		